Excitation functions of the $^{20}Ne + ^{20}Ne$ system

S.P. Barrow, R.W. Zurmühle, J.T. Murgatroyd,* N.G. Wimer, Y. Miao, and K.R. Pohl
Physics Department, University of Pennsylvania, Philadelphia, Pennsylvania 19104

A.H. Wuosmaa, R.R. Betts, M. Freer,† and B. Glagola
Argonne National Laboratory, Argonne, Illinois 60439
(Received 15 July 1994)

A differentially pumped windowless ^{20}Ne gas target and a ^{20}Ne beam produced with the ATLAS accelerator at Argonne National Laboratory were used to measure angle-averaged excitation functions for binary decay of $^{20}Ne + ^{20}Ne$ into low-lying states of $^{20}Ne + ^{20}Ne$ and $^{24}Mg + ^{16}O$, in the region of excitation energy in ^{40}Ca from 51.4 to 58.2 MeV (^{20}Ne beam energies from 61.8 to 75.4 MeV). The $^{20}Ne + ^{20}Ne$ mass partition displays little correlated structure and there exists no evidence of intermediate width resonances in these channels with branching ratios comparable to those seen in the $^{24}Mg + ^{24}Mg$ system. Angular distributions for the elastic channel are consistent with those obtained using optical-model calculations. The excitation functions for the low-lying channels in $^{24}Mg + ^{16}O$ do contain some structures, with widths varying from 400 to 800 keV in the c.m. system.

PACS number(s): 25.70.Ef, 25.70.Hi

I. INTRODUCTION

A recent study of the spin alignment and magnetic substate populations [1] for resonances in the inelastic scattering of the $^{24}Mg(^{24}Mg,^{24}Mg^*)^{24}Mg^*$ [2] system at excitation energies in ^{48}Cr of 59.2 and 60.65 MeV made it possible, for the first time, to compare the actual spins of these resonances with the calculated properties of high spin, high excitation energy states in ^{48}Cr [3–8]. The resonances are consistent with the population of quasimolecular high spin excited states in ^{48}Cr that have large fission partial widths. The spin assignments indicate that the resonating partial waves are 4 units of angular momentum larger than the grazing angular momenta of two spherical $N = Z$, $A = 24$ nuclei. Since there exist few fission channels which can support such high spin, the lifetime of the excited states is long, roughly ten times longer than the transit time of the two ^{24}Mg nuclei. For each resonance, the branching ratios of the elastic and low-lying inelastic channels of $^{24}Mg + ^{24}Mg$ sum to approximately 15% of the total width [9], much larger than would be expected for statistical fission decay.

Theoretical calculations for these quasimolecular configurations in ^{48}Cr suggest that the prolate deformation of the ^{24}Mg ground state is important for the population of molecular configurations in ^{48}Cr, as these configurations resemble two orbiting ^{24}Mg nuclei aligned pole-to-pole. Therefore, the phenomena that dominate the $^{24}Mg + ^{24}Mg$ system are "shape matching" resonances between the $^{24}Mg + ^{24}Mg$ entrance channel and high spin excited states in ^{48}Cr. There has been speculation [1,3,7] that similar structures would be seen in $^{20}Ne + ^{20}Ne$, as ^{20}Ne and ^{24}Mg have comparable ground state prolate deformation. In addition, the large neutron and proton separation energies in ^{40}Ca and ^{48}Cr should reduce the partial widths of the particle evaporation decay from high spin states [7], therefore by default increasing the branching ratios for all other available decay channels, although this has not been verified experimentally.

Other light systems which feature even N, even Z, $N = Z$ so-called "alpha-particle" nuclei have been studied; namely, $^{12}C + ^{12}C$ [10,11], $^{16}O + ^{16}O$ [12], $^{28}Si + ^{28}Si$ [13], $^{32}S + ^{32}S$ [14], and $^{40}Ca + ^{40}Ca$ [15]. The $^{28}Si + ^{28}Si$ system has much structure, some of which are present in several of the decay channels into low-lying excitations of ^{28}Si, but the spins in the $^{28}Si + ^{28}Si$ elastic channel are comparable to the $^{28}Si + ^{28}Si$ grazing angular momentum [16]. Since the ground state of ^{28}Si is not strongly deformed, this result is consistent with the speculation that large prolate deformation is needed to populate long-lived molecular configurations with spins significantly larger than grazing angular momentum. Neither the $^{32}S + ^{32}S$ nor the $^{40}Ca + ^{40}Ca$ systems showed evidence of resonance structures but, again, neither has a large ground state prolate deformation. Much of the early work on $^{12}C + ^{12}C$ and $^{16}O + ^{16}O$ was either a series of single-angle excitation functions or inclusive measurements with γ-ray detectors. The excitation functions reveal pronounced oscillatory structures, but the structures are broad with typical lifetimes comparable to the transit time of the nuclei. Angle-averaged excitation functions in the $^{16}O + ^{16}O$ system suggest that several of the inelastic channels studied [17,18] are dominated by phenomena which are different from the elastic scattering results. Similar conclusions were obtained for

*Present address: Wayne State University, Detroit, MI 48202.
†Present address: University of Birmingham, Birmingham B15 2TT, United Kingdom.

 ©1995 The American Physical Society

some of the inelastic channels in the $^{12}C + ^{12}C$ system [19]. Once again the absence of narrow structures similar to those seen in ^{48}Cr is consistent with the absence of large prolate deformation in the ground state of the reactants. Recently Beck *et al.* [20] performed a series of open channels calculations to compare the number of exit channels available to surface grazing partial waves for several light and medium heavy-ion collisions ranging from $^{12}C + ^{12}C$ to $^{32}S + ^{32}S$. This work concludes that among the reactions studied that feature two *s-d* shell nuclei, $^{20}Ne + ^{20}Ne$ is the most favorable for the observation of resonances, even more favorable than $^{24}Mg + ^{24}Mg$. The number of open channels for grazing partial waves in $^{20}Ne + ^{20}Ne$ is typically an order of magnitude smaller than that for the $^{24}Mg + ^{24}Mg$ system for slightly larger grazing partial waves. The $^{24}Mg + ^{24}Mg$ system is heavier than the $^{20}Ne + ^{20}Ne$ system, which warrants comparing the two systems at different values of the grazing angular momentum.

Previously there has been no comprehensive study of the $^{20}Ne + ^{20}Ne$ system due to the difficulties inherent in using ^{20}Ne as a target and as a tunable beam. With the ECR source serving as injector to the linear accelerator at Argonne National Laboratory, a tunable ^{20}Ne beam has now become available. We recently constructed a differentially pumped windowless ^{20}Ne gas target to complete the equipment needed to study this reaction.

A priori, it is possible that several different mass partitions can support decay from a given resonance configuration in the composite nucleus, as long as each mass partition can support the high spin needed for decay. Of course the fission branching ratios for different binary mass partitions could differ greatly for any given resonance. Studies that include the $^{28}Si + ^{20}Ne$ [9,21] reaction channel indicate the decay of the molecular resonances in ^{48}Cr into the asymmetric mass partitions $^{28}Si + ^{20}Ne$ and $^{32}S + ^{16}O$ is much smaller than the decay into the mass symmetric $^{24}Mg + ^{24}Mg$ mass partition. Study of correlations between different fission channels is not restricted to ^{48}Cr, as, for example, a study of correlations between $^{40}Ca(^{16}O,^{28}Si^*)^{28}Si^*$ and $^{28}Si(^{28}Si,^{28}Si^*)^{28}Si^*$ has also been reported [22]. In the current experiment we have studied $^{20}Ne + ^{20}Ne$ reactions for binary decay into the $^{20}Ne + ^{20}Ne$ and $^{24}Mg + ^{16}O$ mass partitions. We have measured excitation functions in 125 keV steps over a 6.8 MeV center-of-mass energy range from 30.6 to 37.4 MeV, spanning the region from 1.6 to 2.0 times the $^{20}Ne + ^{20}Ne$ Coulomb barrier energy, which is the analogous region to that studied in ^{48}Cr in which the strongest resonances were observed.

II. EXPERIMENT

A windowless differentially pumped gas cell served as the target. The isotopically enriched ^{20}Ne gas was kept at a constant pressure of 10 Torr, which for a 1 cm target length corresponds to a thickness of 12 $\mu g/cm^2$. Two large (1.9 cm by 3.8 cm) rectangular surface barrier solid state detectors positioned on opposite sides of the beam at 40° and 50° measured the energies of the coincident decay fragments. Two apertures were cut into the gas target housing in the recoil plane of the detectors, and covered with 100 $\mu g/cm^2$ thick ^{27}Al foils, which allowed the fragments to exit the target region while still containing the ^{20}Ne gas. A typical decay fragment with an average amount of kinetic energy lost approximately 1 MeV in the ^{27}Al foils. In addition to the energy information, the time-of-flight difference of every coincidence event was also measured. A 1.6 mm inner diameter tantalum collimator 1.27 cm in length allowed the ^{20}Ne beam to enter the target region, and in this way there was little energy degradation of the beam prior to reaching the target. A turbomolecular drag pump collected the ^{20}Ne gas which escaped the target region through the collimator and reintroduced it (after purification it in a sorption pump) back into the target region. This was the first stage of a three-stage recirculation system which enabled us to maintain stable pressure of 10 Torr in the target region over very long time periods with a fixed amount of circulating gas. The turbopumps were mounted directly onto the scattering chamber, and the entire apparatus was very compact and could easily be transported to other facilities. A more comprehensive description of this target assembly will be given in a future publication.

For two body decays, the time-of-flight difference of the decay fragments and kinematics was sufficient to reconstruct the masses of the decay fragments, as well as the center-of-mass angle for the scattering process. The center-of-mass angle was derived from the quantity $\cos(\theta_{\text{c.m.}}) = \alpha(E_L - E_R) + \beta$, where $(E_L - E_R)$ is the difference in the energies recorded by the two detectors. The terms α and β in the calculation are independent of E_L and E_R but are complicated functions of the target mass, the projectile mass, the decay masses, the Q value of the reaction, and the beam energy. In the calculation of the center-of-mass angle, it is important to correct for the energy losses in the ^{27}Al foils. However, for the $^{20}Ne + ^{20}Ne$ mass partition, for center of mass angles near 90°, the energy losses are nearly identical for the two nuclei and therefore cancel in the above calculation. For asymmetric binary decay channels such as $^{24}Mg + ^{16}O$ this is no longer the case. The solid angle of the recoil coincidence was calculated using a Monte Carlo technique [23], as the spatial extent of the gas target over 1 cm in length makes it difficult to calculate the solid angle directly. We note here that the large volume of the target also would have made the use of position sensitive detectors ineffective, as the origin of the reaction within the event region is not defined, and therefore position does not define angle.

The ^{20}Ne gas target was installed at the Argonne National Laboratory ATLAS facility. ATLAS is a pulsed beam linear accelerator and the energy definition of the beam is less than that of a tandem accelerator. In order to study the stability of the centroid and the energy spread of the ^{20}Ne beam we placed an 11 $\mu g/cm^2$ gold foil in the adjustable target mount of an upstream scattering chamber, along with two monitor detectors positioned at $\pm 10°$ relative to the beam. Before and after each run with the gas target we did a brief measurement of the elastic scattering off the gold target. Before the measure-

ments at Argonne, we determined the monitor detector resolution for ^{24}Mg and ^{16}O using beams from the University of Pennsylvania Tandem Accelerator scattered off a gold target of comparable thickness, and interpolated the expected full width at half maximum (FWHM) for a monoenergetic ^{20}Ne beam, which was found to be 185 keV for a 70 MeV ^{20}Ne beam energy. At Argonne, a typical monitor spectrum had an energy FWHM of 500 keV, about 2.7 times larger than the expected detector resolution for a monoenergetic ^{20}Ne beam, which thus yields an estimate of the intrinsic beam energy spread (FWHM) of ~450 keV, or ~225 keV in the center-of-mass system. Based on a comparison of the gold target elastic events done before and after each run with the ^{20}Ne target, there was little variation in the centroid or the width of the beam energy for any of the beam energies used in this work.

We also used the gold elastic scattering measurements to establish a relative energy calibration of ATLAS and University of Pennsylvania Tandem Accelerator. A pulser was used to simulate the average of the pulse heights of the monitor detector energy signals for known beam energies of ^{24}Mg and ^{16}O beams from the Tandem accelerator scattering off a gold target, and the same pulser with the same settings was then used to calibrate the ^{20}Ne pulse heights after scattering off the gold target during the experiment at Argonne. An additional check of the energy calibration was performed using the ^{20}Ne(^{20}Ne,^{16}O)^{24}Mg reaction. The narrowest structure observed in this reaction has a width (FWHM) of approximately 400 keV in the c.m. frame. We determined the centroid energy and the width of the same resonance in the time reversed reaction using a 30 μg/cm^2 ^{24}Mg target and a ^{16}O beam from the University of Pennsylvania Tandem Accelerator. The centroid energy was 405 keV lower than the energy derived from the calibration of the ATLAS accelerator, and that amount was subtracted from all ATLAS center-of-mass energies prior to plotting the excitation functions. For both measurements, the resonance had nearly identical shape and width, which suggests that 400 keV is the actual width of the structure.

III. ANALYSIS AND RESULTS

A typical time-of-flight difference spectrum (DT) is shown in Fig. 1(a). Only coincidence events in which the sum of the two coincident energy signals corresponded to a reaction Q value greater than -30 MeV were included in Fig. 1(a). This restriction excluded many-body decay events in which only two of the fragments struck the detectors. Each peak in Fig. 1(a) corresponds to one binary decay configuration. The width (FWHM) of the ^{20}Ne + ^{20}Ne partition is 580 ps. For the two strongest mass partitions Q-value spectra were generated by summing the energy signals in the two detectors, and are shown in Figs. 1(b) and 1(c). The counts in the peaks marked with arrows in Figs. 1(b) and 1(c) were then summed, and after proper normalization, plotted as a function of excitation energy in ^{40}Ca, as well as the center-of-mass

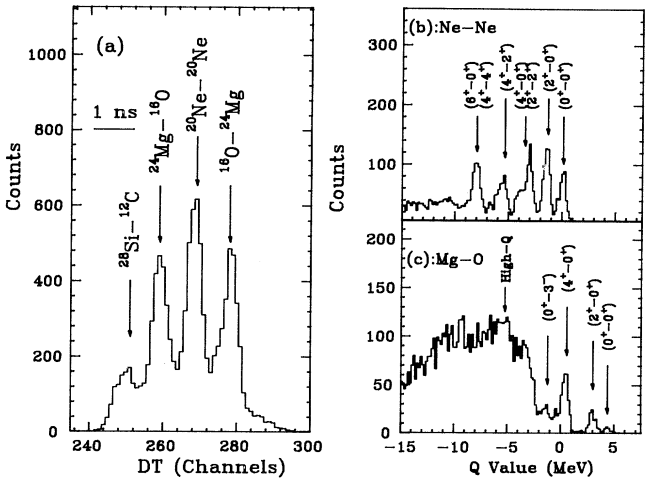

FIG. 1. Mass partitions and Q spectra for the current work. The 1 ns bar in 1(a) indicates one nanosecond.

energy of the entrance channel. In order to reduce the sensitivity to direct reaction contributions to the cross section, which dominate the yield at forward angles, the most forward angle data were excluded from the elastic and inelastic excitation functions discussed in the current work. Center-of-mass angles between 76° and 103° were included in the excitation function for the elastic channel.

The excitation functions for the exit channels labeled in Fig. 1(b) are shown in Fig. 2. The characteristic cross

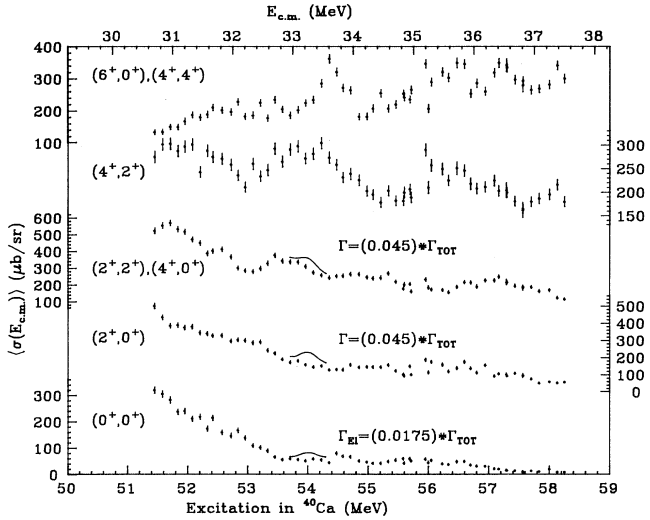

FIG. 2. Angle-averaged excitation functions of ^{20}Ne + ^{20}Ne for the elastic and several inelastic channels. The x axis is labeled with the excitation energy in ^{40}Ca at the bottom and with the entrance channel center-of-mass energy on top. The center-of-mass angle range for the elastic channel is approximately 76°–103°. The solid curves denote the shape and strength of a Breit-Wigner resonance analogous to those seen in the ^{24}Mg + ^{24}Mg system. The error bars are statistical.

section of the elastic channel is approximately 100 μb/sr. This value is about two times larger than the characteristic angle-averaged elastic cross sections in the ^{28}Si + ^{28}Si and ^{32}S + ^{32}S systems averaged over comparable center-of-mass angle ranges, and five times larger than the ^{24}Mg + ^{24}Mg nonresonant elastic cross section, for center-of-mass energies of comparable multiplicative constants times the respective Coulomb barriers. The elastic and low-lying inelastic channels show little energy dependence other than a monotonic decrease with increasing beam energy. Higher excitations do contain some structures. To assess the significance of these structures, we have assumed the presence of a resonance in ^{40}Ca at 54.0 MeV of excitation with a total width of 300 keV in the c.m. system and a spin of $J = 32$ (the calculated grazing angular momemtum for ^{20}Ne + ^{20}Ne at this beam energy using the parameters listed in Table I is 26), with branching ratios into low-lying states of ^{20}Ne + ^{20}Ne identical to the branching ratios in ^{24}Mg + ^{24}Mg. Then, under the further assumption of incoherent superposition on the background, we can estimate the energy dependence of the cross section for a 250 keV center-of-mass square averaging interval ^{20}Ne beam spread. For the current experiment, based on the geometry of the gas target and the c.m. angle regions studied, the resonance would manifest the shape and strength indicated by the solid lines in Fig. 2. The nonresonant background in the current work is larger than that for ^{24}Mg + ^{24}Mg, which makes the signal-to-background ratio for the hypothesized Breit-Wigner resonance at 54.0 MeV of excitation less than that for the ^{24}Mg + ^{24}Mg resonances, and the smoothing of the Breit-Wigner resonance cross sections due to the energy spread of the beam further reduces the sensitivity of this experiment. We estimate that the current work is not sensitive to Breit-Wigner resonances with an entrance channel partial width less than approximately 1% of the total width. Therefore, we can only state that there is no evidence of correlated resonance structure with an elastic branching ratio greater than 1%.

For each point in the excitation function, we are able to extract the angular distribution of the elastic channel. The angular distributions in 1 MeV steps in the center-of-mass system are shown in Fig. 3, along with optical-model fits using the parameters listed in Table I. The parameters were determined by requiring good agreement between the fits and the angular distributions for the most forward angles. For the angular distributions at excitation energy = 55.7, 56.8, and 58.0 MeV, two adjacent energies in the excitation function separated by approximately 125 keV were included to improve the statistics. The angular distributions are in qualitative agreement with the optical-model calculations.

We are able to adjust the angle range over which

TABLE I. Optical-model parameters for the elastic scattering angular distributions.

V_0 (MeV)	r_0 (fm)	a (fm)	W (MeV)	r_0' (fm)	a' (fm)	r_{0C} (fm)
38.0	1.140	0.642	12.00	1.166	0.659	1.20

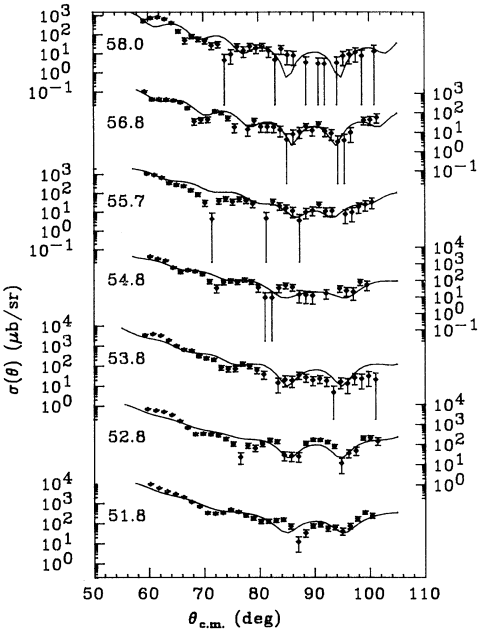

FIG. 3. Elastic scattering angular distributions for ^{20}Ne + ^{20}Ne. The excitation energy in ^{40}Ca is listed to the left of each angular distribution. The solid lines are optical-model calculations using the parameters listed in Table I. The error bars are statistical.

the excitation function is averaged during playback by putting restrictions on the kinematics of the two fission fragments. Using this procedure, we obtained 90°±2° excitation functions for the elastic channel (0^+,0^+) and for single excitations to the first 2^+ state in ^{20}Ne (2^+,0^+). The results are shown in Fig. 4(a). The elastic chan-

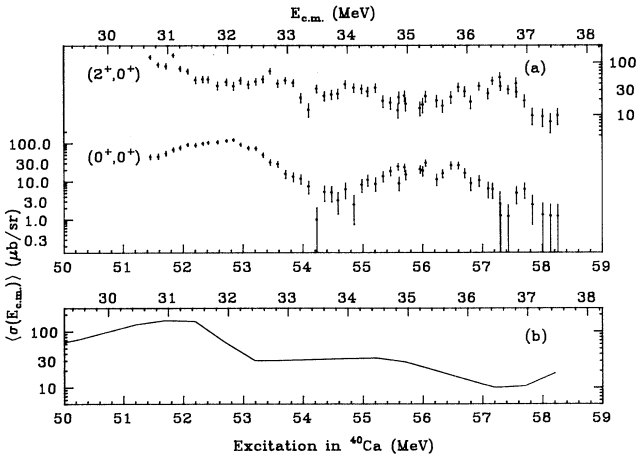

FIG. 4. Excitation functions for a narrow angle range $\theta_{c.m.}$=90°±2° for single excitation to the lowest lying 2^+ state in ^{20}Ne + ^{20}Ne (2^+,0^+) and for the elastic channel (0^+,0^+). The x axis is labeled with the excitation energy in ^{40}Ca at the bottom and entrance channel center-of-mass energy on top. Also shown is a $\theta_{c.m.}$=90° optical-model calculation excitation function using the same parameters as Table I, except for W, which has a value of 8 MeV for the calculations plotted in this figure. The error bars are statistical.

nel results differ substantially from the angle-averaged excitation functions, and show pronounced structures. Optical-model calculations such as the one shown in Fig. 4(b) produce similar pronounced oscillations in the 90° excitation function for very shallow complex wells ($W \sim 8.0$ MeV). The $(2^+,0^+)$ excitation function for the narrow angle range of 90°±2° shows no similar structures.

The positive-Q value of the $^{24}Mg + ^{16}O$ mass partition makes it possible, based on optical-model calculations using the parameters listed in Table I, for this mass partition to support as much grazing angular momentum as the $^{20}Ne + ^{20}Ne$ entrance channel for a given ^{40}Ca excitation energy. It therefore is possible that these two mass partitions are able to share decay from high spin configurations in ^{40}Ca since they are angular momentum matched. The excitation functions for the $^{24}Mg + ^{16}O$ mass partition are shown in Fig. 5. There is clearly more structure here, some of which, such as at excitation energy =53.0 and 57.3 MeV, is present in several of the low-lying excitations of ^{24}Mg. More weakly correlated structures are present at excitation energy =53.8, 54.8 and possibly 55.6 and 56.6 MeV. These structures clearly demonstrate that the energy definition of the ^{20}Ne beam used in this experiment is sufficiently small to observe intermediate width resonances in these excitation functions. The positive Q-value exit channels have small cross sections, so even if the correlated structure at 53.0 MeV were some type of resonance in ^{40}Ca, the branching ratios probably still would sum to a total much less than the 15% observed in ^{48}Cr. For example, using the quoted 1% upper limit for the elastic channel branching ratio, then the resonance at 53.0 MeV of excitation in the mutual ground state of the $^{24}Mg + ^{16}O$ mass partition would have an exit channel branching ratio of 0.184%,

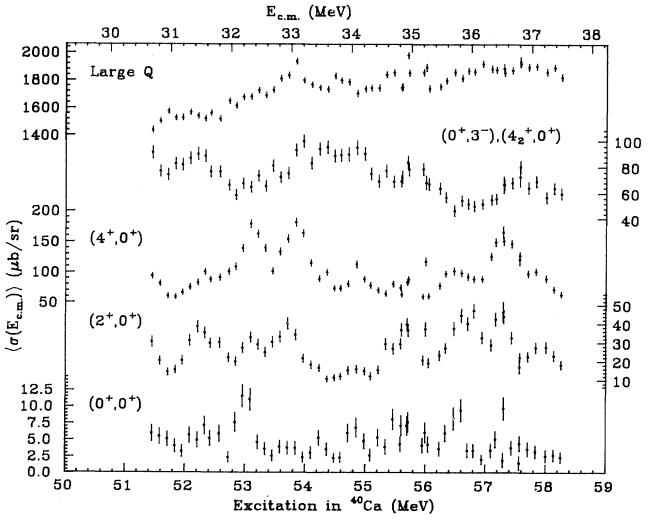

FIG. 5. Angle-averaged excitation functions for the $^{24}Mg + ^{16}O$ exit channel. The x axis is labeled with the excitation energy in ^{40}Ca at the bottom and entrance channel center-of-mass energy on top. The center-of-mass angle range for the $(0^+,0^+)$ channel is approximately 48°–99°. The error bars are statistical.

assuming $J = 32$. This number is similar to the branching ratios from the ^{48}Cr molecular configurations into the $^{28}Si + ^{20}Ne$ mutual ground state [9].

The elastic and inelastic scattering of the $^{16}O + ^{24}Mg$ system has previously been studied extensively [24–26]. However, all of the excitation functions measured were at lower excitation energies in ^{40}Ca, and were for a single angle, which makes direct comparison with the angle averaged excitation functions of the present work difficult, as is illustrated by comparing the angle averaged and 90°±2° excitation functions of the elastic channel for the current work. Much structure with widths on the order of 1 MeV has been seen in the $^{16}O + ^{24}Mg$ single-angle excitation functions. There has been no previous study of angle-averaged excitation functions for the transfer reaction $^{24}Mg(^{16}O,^{20}Ne^*)^{20}Ne^*$.

Comparing the current work with other experiments that studied scattering of identical $N = Z$ even nuclei, the results most strongly resemble those for the $^{32}S + ^{32}S$ and $^{40}Ca + ^{40}Ca$ systems, in which no evidence of correlated resonance structure was observed, although the other two measurements were sensitive to smaller elastic branching ratios than is the current work.

IV. SUMMARY AND CONCLUSION

Based on the results of the angle-integrated excitation functions, and the elastic scattering angular distributions, we conclude that quasimolecular resonances with elastic branching ratios greater than 1% are not being populated in the current work. The results for smaller elastic branching ratios are inconclusive. The excitation functions for the $^{20}Ne + ^{20}Ne$ mass partition contain no structures common to more than one exit channel, the angular distributions and the 90° elastic scattering excitation function are consistent with optical-model calculations, and there is no evidence of partial waves larger than the grazing angular momentum of two $N = Z$, $A = 20$ spherical nuclei having appreciable cross sections. However, the reaction cross sections in the current work are larger than those seen in $^{24}Mg+^{24}Mg$, and the beam energy spread in our measurement was approximately 450 keV FWHM in the laboratory system, and either or both of these two factors could reduce our sensitivity to intermediate width resonant phenomena that possess elastic branching ratios smaller than 1%. The $^{24}Mg + ^{16}O$ mass partition shows more structure, some of which are correlated among low-lying excitations in ^{24}Mg, but the cross sections for the low-lying excitations in this transfer channel are small.

There has been speculation that the large prolate deformation in ^{24}Mg is important for the observation of the ^{48}Cr molecular configurations. The present work suggests that large prolate deformation is not sufficient, and that the shape matching between the $^{20}Ne + ^{20}Ne$ entrance channel and the high spin excited states in ^{40}Ca is not as good as that between the $^{24}Mg + ^{24}Mg$ entrance channel and the high spin excited states in ^{48}Cr. Two of the nuclear structure models [3,5] suggest that the high spin states in ^{40}Ca do not have deformations comparable

to the deformations of the molecular states in ^{48}Cr. This conclusion will be discussed in more detail in a future publication, which will also include the results of studies we made of the ^{28}Si + ^{20}Ne and the ^{24}Mg + ^{20}Ne systems. It is interesting that the nonresonant background in the elastic and inelastic channels is so much larger than what was observed in ^{24}Mg + ^{24}Mg and the other systems in this mass region studied to date. In a recent paper Beck *et al.* [20] argued that the smaller the number of open channels in a given system, the greater the probability that resonance phenomena will be observed. On that basis they predict strong resonance structure for ^{20}Ne + ^{20}Ne, and our results represent a departure from this picture. The small resonant cross sections for the structures seen in the ^{24}Mg + ^{16}O exit channels could be consistent with a small entrance channel partial width. If this were so, the branching ratios for the ^{24}Mg + ^{16}O exit channel would probably sum to a few percent, which is characteristic of the decay strength of the molecular resonances in ^{48}Cr into the asymmetric ^{28}Si + ^{20}Ne mass partition. As of this writing there still is no indication of nuclei in this mass region which possess strongly correlated resonant structures with spins 4 units of angular momentum larger than the grazing angular momenta values other than in ^{48}Cr.

ACKNOWLEDGMENTS

We would like to thank H.T. Fortune and C. Lee for helpful discussions. This work was supported by the National Science Foundation. The work of the Argonne National Laboratory Physics Division is supported by the U.S. Department of Energy, Nuclear Physics Division, under Contract No. W-31-109-Eng-38.

[1] A. W. Wuosmaa, R. W. Zurmühle, P. H. Kutt, S. F. Pate, S. Saini, M. L. Halbert, and D. C. Hensley, Phys. Rev. C **41**, 2666 (1990).
[2] R. W. Zurmühle, P. H. Kutt, R. R. Betts, S. Saini, F. Haas, and O. Hansen, Phys. Lett. **129B**, 384 (1983).
[3] D. C. Zheng, L. Zamick, and D. Berdichevsky, Phys. Rev. C **42**, 1004 (1990).
[4] R. Maass and W. Scheid, Phys. Lett. B **202**, 26 (1988).
[5] W. D. M. Rae and A. C. Merchant, Phys. Lett. B **279**, 207 (1992).
[6] R. Maass and W. Scheid, J. Phys. G **18**, 707 (1992).
[7] A. H. Wuosmaa, Dissertation, University of Pennsylvania, Philadelphia (1988).
[8] E. Uegaki and Y. Abe, Phys. Lett. B **231**, 28 (1989).
[9] S. Saini, R. R. Betts, R. W. Zurmühle, P. H. Kutt, and B. K. Dichter, Phys. Lett. B **185**, 316 (1987).
[10] D. A. Bromley, J. A. Kuehner, and E. V. Almqvist, Phys. Rev. **123**, 878 (1961).
[11] E. Almqvist, D. A. Bromley, J. A. Kuehner, and B. Whalen, Phys. Rev. **130**, 1140 (1963).
[12] M. L. Halbert, F. E. Durham, and A. van der Woude, Phys. Rev **162**, 899 (1967).
[13] S. Saini and R. R. Betts, Phys. Rev. C **29**, 1769 (1984).
[14] P. H. Kutt, S. F. Pate, A. H. Wuosmaa, R. W. Zurmühle, O. Hansen, R. R. Betts, and S. Saini, Phys. Lett. **155B**, 27 (1985).
[15] R. R. Betts, in *Nuclear Physics With Heavy Ions*, edited by P. Braun-Munzinger (Harwood Academic, New York, 1984).
[16] R. R. Betts, S. B. DiCenzo, and J. F. Peterson, Phys. Lett. **100B**, 117 (1981).
[17] S. P. Barrow, R. W. Zurmühle, A. H. Wuosmaa, and S. F. Pate, Phys. Rev. C **46**, 1934 (1992).
[18] S. F. Pate, R. W. Zurmühle, A. H. Wuosmaa, P. H. Kutt, M. L. Halbert, D. C. Hensley, and S. Saini, Phys. Rev. C **41**, R1344 (1990).
[19] S. F. Pate, R. W. Zurmühle, P. H. Kutt, and A. H. Wuosmaa, Phys. Rev. C **37**, 1953 (1988).
[20] C. Beck, Y. Abe, N. Aissaoui, B. Djerroud, and F. Hass, Phys. Rev. C **49**, 2618 (1994).
[21] S. P. Barrow *et al.* (to be submitted).
[22] B. K. Dichter, P. D. Parker, S. J. Sanders, R. R. Betts, and S. Saini, Phys. Rev. C **35**, 1304 (1987).
[23] S. P. Barrow, Dissertation, University of Pennsylvania, 1994.
[24] M. Paul, S. J. Saunders, D. F. Geesaman, W. Henning, D. G. Kovar, C. Olmer, J. P. Schiffer, J. Barrette, and M. J. LeVine, Phys. Rev. C **21**, 1802 (1980).
[25] A. L. Szily, R. L. Filho, M. M. Obuti, J. M. Oliveira, O. P. Fihlo, W. Sciani, and A. C. C. Villari, Phys. Rev. C **40**, 681 (1989).
[26] B. R. Fulton, J. S. Lilley, T. M. Cormier, and P. M. Stwertka, Phys. Rev. C **27**, 1811 (1983).